Anderson-Schulz-Flory Product Distribution – Can it be Avoided for Fischer-Tropsch Synthesis?

Burtron H. Davis
Center for Applied Energy Research
University of Kentucky
2540 Iron Works Pike
Lexington, KY 40511

Prepared for Presentation at the AIChE 2003 Spring National Meeting, New Orleans, LA
March 30 - April 3, 2003, Historical Development of the Fischer-Tropsch Synthesis Process - I

INTRODUCTION

The Fischer-Tropsch Synthesis may be viewed as a simple polymerization reaction, the monomer being CO or a C_1 species derived from it. Schulz (1,2) derived an equation for the distribution of molecular weights of polymers obtained by a free radical polymerization process, that is, through a one-by-one addition of monomer to a growing chain. The Schulz distribution function is applicable generally if there is a **constant** probability of chain growth, α, and α < 1; the latter requirement applies when some reaction limits the chain growth. The probability for chain growth, α, is defined as:

$$\alpha = r_P/(r_P + \Sigma r_t) \quad \textbf{[1]}$$

where r_p is the rate of chain propagation and r_t is the rate of chain transfer or chain termination. The probability of the chain growth step to take place P times without termination is

$$P_p = \alpha_1 \alpha_2 \alpha_3 \ldots \alpha_p = \alpha^P \quad \textbf{[2]}$$

The number of molecules per degree of polymerization P, n_p, is proportional to the probability of their formation

$$n_p = const\ \alpha^P \quad \textbf{[3]}$$

The mass fraction m_p is proportional to n_p as well as the molecular weight of the components of the fraction ($M_p = M_M P$, where M_M is the molecular weight of the monomer)

$$m_p = AP\alpha^P \quad \textbf{[4]}$$

where A contains the constant M_M. The mass fraction is defined so that

$$\Sigma m_p = 1 \quad [5]$$

The mass fraction is considered to be a continuous function so that

$$\int_o^\infty m_p dP = A \int_o^\infty P\alpha^P dP = 1 \quad [6]$$

and

$$A = 1/\int_o^\infty P\alpha^P dP \quad [7]$$

Solving the integral ($\alpha < 1$, $\alpha^\infty = 0$) and combining equations [4] and [7] leads to

$$m_p = (ln^2\alpha)P\alpha^P \quad [8]$$

Rearranging gives the more familiar form

$$\log(m_p/P) = \log(ln^2\alpha) + (\log\ \alpha)P \quad [9]$$

Thus, a plot of log (m_p/P) versus P should result in a straight line.

Flory published a number of theoretical distribution functions for this and other types of macromolecular formation (e.g., reference 3). Thus, polymer scientists usually designate distributions as represented by [9] as conforming to a Schulz-Flory distribution.

Similar equations were derived, apparently independently, by catalysis scientists (4-6). Anderson continued his efforts to develop chain growth mechanisms and to account for the products formed by chain branching (7). Many catalysis scientists therefore recognize Anderson's contributions to the Fischer-Tropsch Synthesis by designating equation [9], and plots based upon it, as an Anderson-Schulz-Flory (ASF) equation or plot, and we shall follow this practice.

Possible Deviations from ASF

There are three possibilities for ASF distributions. In the first case, all of the products follow an ASF distribution. In the second case, the products follow an ASF distribution up to some carbon number and then a dramatic negative deviation occurs (a deviation where the experimental value is much lower than predicted for an ASF distribution). In the third instance, the products follow an ASF distribution up to some carbon number and then there is a gradual positive deviation of the products to eventually follow a second ASF distribution. In the third case, the second alpha value must be higher than the first alpha value. The latter two cases will be discussed below since the first instance is the one that is expected.

Another possibility is that an excess of low carbon number products, based on ASF, are formed; claims of this type are not as common. The maximum C_2-C_4 products, based on ASF, is 57%. German patents (8) reported up to 89% C_2-C_4 products, including a much lower concentration of methane than predicted by ASF. However, the C_2-C_4 products conformed to an ASF distribution (9). Other reports from BASF did not show this unusual behavior. Unusual distributions reported from the Exxon labs were also considered in the report by the Catalytica Associates authors. Madon et al. (10-12) reported product distributions (excluding light products) that showed a sharp, narrow peak with one or more shoulders. Modeling by Catalytica Associates,Inc. of heavy product holdup in the reactor and traps

produced a similar distribution (13), with the implication that experimental artifacts produced the unusual results.

Chain Limiting (Cut Off)

Chain limiting, as used in the literature, may be divided into two broad categories. In many instances, the definition has not been given and considerable misunderstanding has resulted from the use of chain limiting.

Low Alpha Distribution

In the first category, the products are low molecular weight but follow a normal ASF distribution, or may have a slight positive deviation. This distribution is required for operation in a fluid bed reactor. If liquid products are formed in the fluid bed reactor, either circulating as used initially at Sasol or fixed fluid as used in the commercial plant at Brownsville, Texas, catalyst particles will adhere to each other and eventually become so large that they cannot be fluidized. Thus, some reports have used chain limiting to mean that liquid products are not formed in amounts to allow a liquid phase to form. This is the type of operation that is practiced by Sasol for about 90% of their production (first in fluid bed and now fixed fluid bed reactors) and the one used by Mossgass. However, in general the products do not deviate significantly from a single ASF distribution. Thus, this case should not be considered as an abnormal distribution that deviates from the normal ASF polymerization mechanism. This is just a low alpha ASF distribution and should not be considered to be produced by a chain limiting FTS mechanism.

Bifunctional Catalysis

The combination of FT synthesis with cracking or hydrocracking processes was commonly practiced in Germany during the 1930-1940 period; however, the two operations were obtained in separate processes. Obviously, cracking the heavier products to low molecular weight products can cause deviations from ASF. To our knowledge, the first to attempt to conduct the two processes in a single reactor were Gulf workers in the 1970s (14). They conducted the synthesis with a mixed bed of cobalt catalyst and a silicate cracking catalyst; the product distribution deviated from ASF. Mobil Oil workers conducted extensive studies in which they attempted to effect bifunctional catalysis in one reactor (15); eventually they settled on separate reactors for the two processes. Separate processes are also utilized at the commercial plant operated by Shell Middle Distillate Synthesis (16). However, the deviation from ASF is artificially introduced by cracking of heavier hydrocarbons and is not a deviation from the FT synthesis.

Negative Deviation from ASF

Until recently, the goal of the FTS synthesis has been to produce gasoline range compounds as the major product. At the same time, it was desirable to limit the amount of light gases, C_1 to C_4 compounds, since there was not a great demand for these products in most locations. It was therefore desirable to have the products resemble a bell-shaped type curve that had a maximum at about C_7-C_8. In other words, it was desirable to have the ASF distribution show a negative deviation from ASF up to about C_4 and to then cut-off abruptly above about C_{11}. While reports showing negative deviations for the lower carbon number products are absent, or very limited, many reports of negative deviations of the higher carbon number products have appeared. The following section considers some of these claims for negative deviations.

With the increased interest in FT synthesis following the energy crisis in the 1970s, many groups became active in FT. By then the usage of zeolites, starting with the discovery by Mobil workers of the improved catalytic cracking selectivity, had increased dramatically. It was predictable that many groups would use zeolites as supports for the FT synthesis, and this was the case. The use of these supports led to reports of chain limiting FT synthesis.

A number of "Client Private" reports on a range of topics were offered during the 1970-1980 period by Catalytica Associates, Inc. The circulation of these reports was restricted to multiclients but some of the copies were later sold at a significantly reduced price without these restrictions. In 1980, a report provided their recent thoughts on Schulz-Flory limitations and violations in CO-H_2 reactions. They considered that the broad range of products produced by the FT synthesis presented experimental problems that can hinder an accurate determination of product distribution. Included amont these reasons were: (1) condensation of products in catalyst and/or reactor; (2) condensation in downstream piping; and (3) errors associated with the use of multiple product collection traps.

Among the first, if not the first, to show unusual chain limiting product distribution obtained using the zeolite support were Vanove, et al. (17) and Nijs et al. (18). Ballivet-Tkatchenko, et al. (19) also reported that FT synthesis could be "tailored" by the use of iron, cobalt and ruthenium carbonyl complexes deposited on faujasite Y-type zeolites so that only short (C_1-C_9) chain hydrocarbons were produced. These latter authors reported that, while it appeared that the small metal particles needed to be stabalized in the zeolite supercage, it was not clear whether the chain limitation was due to the small metal particle size or the shape selectivity imposed by the zeolite. Frankel and Gates (20) reported that catalysts prepared by reduction of Co(II) ions exchanged into A- and Y-zeolites with cadmium metal vapor were unique. The A-zeolite catalyst produced propene as the only hydrocarbon product. The Y-zeolite based catalyst also showed non-ASF hydrocarbon distributions which were characterized by almost no C_2 and C_3 hydrocarbons and the C_4-C_7 mixture making up about 70% of the hydrocarbon products.

Jacobs and van Wouwe (21) reviewed work that showed non-ASF distributions up to 1982 and indicated that the ultimate proof of the validity of the data had to come from the authors of the various papers. Later work by the Jacobs group (22) presented data for three iron Y-zeolite catalysts. Only one of these catalysts retained the iron in the interior of the zeolite while the iron in the other two catalysts was located almost exclusively on the exterior of the zeolite particles. The two catalysts with the iron on the exterior of the catalyst particles produced products that fit the ASF distribution (Figure 1). With the catalyst that initially contained the iron in the interior zeolite pores, the product distribution initially showed a cut-off at about carbon number 8. However, as the time on stream increased the cut-off occurred at higher carbon numbers, the growth factor steadily increased, and by 120 hours on stream the product distribution has changed to the normal two-alpha plot (Figure 2). These authors assumed that the sites responsible for the first growth mechanism (α_1) is associated with the zeolite supported Fe_2O_3 phase and those giving the α_2 growth rate occurs with the extrazeolite large Hägg-type carbide. The data in Figure 2 are what are anticipated if there is holdup of the heavier products within the zeloite pores. However, if this is the case for the data in Figure 2, the small crystallites in the zeolite must have a lower chain growth probability than the larger crystallites do.

Gates and coworkers published several papers that emphasized the characterization of a variety of metal clusters loaded onto and into zeolite structures; for a number of these catalysts FT synthesis was used as the reaction to relate to the characterization data (e.g., 23-28). In general, the clusters tested had a lower activity than normal FT catalysts. The reaction was conducted in a fixed bed reactor and the products were conducted from the reactor to the g.c. through a heated (about 149^{o}C) line. Products were normally reported through five carbon numbers. Several of the clusters produced products that were reported to be non-ASF; the results in Figures 3 and 4 are representative. When the products are analyzed through higher carbon numbers (e.g., through carbon number 70) some or all of the lower carbon number products show slight deviations from ASF. However, when the analysis is conducted on products up to carbon number 70, the C_1-C_5 products are a small fraction of the total products and the deviation, apart from C_2, is usually not emphasized. However, when the product fraction is only in the range C_1-C_5, these deviations are magnified to a major extent. At least some of the non-ASF features of the data reported by Gates and coworkers are due to the limited range of hydrocarbons that were analyzed. In support of this view, plots that were considered to show ASF distributions also exhibited similar deviations but not to the same extent (Figure 5)(28).

Yang et al (29) report that the negative deviation from ASF distribution is caused by the cut-off effect of small particle size catalyst particles. Wells et al (30) conducted FT synthesis at low pressure using two Co/MnO catalyst formulations and found that the main products were alkenes, principally propene, with minimum methane, demonstrating that the catalyst was chain limiting in the FT synthesis route.

The above is not a comprehensive review of all literature relating to cut-off or chain limiting FT synthesis but is intended to give a flavor of the character of the claims and the type of results obtained over the past 25 years. In the author's view, essentially all of the papers reviewed were based on data obtained under conditions that were not obtained under steady state conditions; that the analysis was conducted under conditions that led to a cut-off; and/or the product distribution was obtained over such a small carbon number range that it magnified minor deviations from ASF.

Yang et al. (31) reported that previous studies indicated that the length of the growing chain was limited by the dimension of the metal crystallite (17,32-37) and developed a theoretical model based on this concept. Thus, on metal crystal surfaces the products followed a normal ASF distribution so long as the crystal face exceeded some minimum size but below that size the chain length decreased very rapidly beyond some carbon number. They represented the chain propagation on large crystals by the normal ASF equation:

$$\phi_n = \phi_1 \alpha^{n-1} \quad \textbf{[10]}$$

where ϕ_n is the mole fraction of product containing n carbons and α is the probability of chain growth. They then imposed a size distribution function, $q(A_n)$, where A_n is an area of a given size, on the ASF formula:

$$\phi_n = \phi_1 \alpha^{n-1} q(A_n) \quad \textbf{[11]}$$

or

$$\log(\phi_n) = \log(\phi_1) + (n-1)\log(\alpha) + \log(q(A_n)) \quad \textbf{[12]}$$

The term $\log(q(A_n)$ modifies the normal ASF distribution so that the predicted ASF plot will resemble that shown in Figure 6. They utilized data from three references (35-37) to show good agreement between the experimental results and their theoretical prediction. Representation of this agreement is shown in Figure 7 using data from reference (36). However, the products from the synthesis were transmitted to the gas chromatograph through a heat traced line kept at a temperature that would provide the cut-off shown in Figure 7. The same limitations appear to be able to account for the cut-off of the product distribution in the other two data sets used by Yang et al. Thus, the agreement of the data with the theory does not support the theory since the cut-off of products is due to limitations of the analytical procedure, and not the synthesis mechanism.

Another feature that was considered to offer the possibility of limiting the extent of chain growth was a special confinement due to limited accessibility of the site. Placing a metal particle in the cage of a zeolite offered one means of limiting the space surrounding the catalytic particle. However, it is difficult to differentiate the impact of shape selectivity imposed by the zeolite structure independent from the impact of the crystal size.

In spite of the experimental difficulties that must be overcome to be sure that the chain limitation is not due to experimental artifacts, reports of negative deviations from ASF still appear, frequently with poorly described experimental details. Ungar and Baird (38) obtained shape selectivity using cobalt in NaY zeolite catalysts with a cut-off at C_8. In a private communication (39), these authors indicate that the cut-off is likely due to adsorption of the heavier products in the pores of the zeolite; however, it does not appear that these authors published the data other than what was reproduced in the private communication. Vanhove et al. (40) reported a chain limiting distribution and indicated that this could be due to a long residence time of the heavier products in catalyst pores and their hydrocracking to lighter products because of the long residence time. These authors also indicated that the non-ASF distributions were only obtained at low loadings of the catalytic component; at higher loadings the products from the larger catalyst particles produced ASF distributions and these covered up the non-ASF products. McMahon et al. (41) found a tailoff in the ASF plots at the C_6-C_9 range, indicating a shape selective effect of the zeolite support. The tailoff was observed at all temperatures used and was not due to product accumulation in the pores, as indicated by the inability to extract heavier hydrocarbons from the spent catalyst. The data of these authors were obtained at atmospheric pressure, and this is a feature that is common to many of the reports of tailoff. Lee and Ihm (42) found a normal ASF distribution for zeolite catalysts prepared by ion exchange. decided non-ASF, with a preferencne for C_3 and C_4 hydrocarbons, was obtained for a catalyst prepared using a carbonyl complex impregnation method. Ozin and coworkers (43-45) found a decided selectivity for butene from CO hydrogenation using very small iron clusters within the cages of faujasite zeolites; again, the studies were at one atmosphere operating pressure.

Many of these deviations can be accounted for by aldol type reactions of the aldehydes and/or ketones that are present for low pressure operations.

Two ASF Distributions

Anderson (46) summarized product distribution results up to about 1954. Included in this review were the results of the Schwarzheide tests using catalysts from Lurgi, Brabag, K.W.I., I.G. Farben, Ruhr Chemie, and Rheinpreussen as well as tests at the larger U.S. pilot plants, and Standard Oil Co. of New Jersey (Figure 8). These results included operations with iron catalysts both in fixed and fluidized reactors. The results in Figure 8 clearly indicate that a single α value does not adequately describe the data. Up to carbon number 9 to 11 the data fit one alpha value for equation [9] very well; however, a second α value is needed to describe those products higher than carbon number 9 to 11. These early workers did not have the benefit of gas chromatography to analyze the higher molecular weight products. Thus, while Anderson noted the need for two or more alpha values to describe the products from FTS using iron catalysts, it received little attention. Furthermore, FTS products from a cobalt catalyst were adequately described with a single alpha value.

Madon and Taylor (47) conducted extensive tests with a precipitated, alkali-promoted iron-copper catalyst. They reported a product distribution for the condensed products from FTS using a plug flow reactor that exhibited a two-alpha plot (Figure 9) but the break occurred at a higher carbon number than those in Figure 8. Madon and Taylor (47) noted that Anderson and coworkers (48) had obtained such a plot but with the break occurring at a lower carbon number. Madon and Taylor noted that Hall et al. (49) had suggested that in addition to stepwise growth with a single carbon intermediate, multiple build-in of growing chains could occur and that this could affect the growth rate of heavy hydrocarbons. Madon and Taylor, after considering this explanation, suggested instead that chain growth takes place on at least two types of sites, each having a slightly different chain growth probability α.

Novak et al. (50) considered the impact of readsorption of α-olefins upon the products from a continuous stirred tank reactor (CSTR) and a plug flow reactor (PFR). They also considered that α-olefins could only initiate chain growth, or that they can also isomerize to internal olefins as well as be hydrogenated. For the CSTR, these authors concluded that, even with such secondary reactions, the products still exhibit an ASF plot. For the PFR, the products deviate from an ASF plot when α-olefins can undergo only chain initiation. If, however, as is the case in a more realistic situation, the α-olefin also undergoes hydrogenation and isomerization in addition to chain initiation, the distribution rapidly becomes similar to an ASF distribution. Finally, these authors considered the case where the chain growth parameter was allowed to vary along the length of a PFR by forcing the C_1 surface concentration to vary and found, in this case also, that the distribution is quite close to a Flory distribution.

Satterfield and Huff (51) initially concluded that the products for a doubly promoted catalyst (C-73, United Catalysts, Inc.) in a CSTR yielded a precise linear relationship between the log of the mole fraction of the products and the carbon number as predicted by an ASF distribution provided all products, including oxygenate species, were included. The linear relationship held over four orders of magnitude of the moles of products and for carbon numbers from 1 to about 20 over a wide range of gas compositions. The chain growth probability factor, α, increased slightly from 0.67 at 269°C to 0.71 at 234°C.

Huff and Satterfield (52), after re-examination of their previous data and a consideration of new experimental data on three different iron catalysts, reported that in some cases, the ASF distribution plot can only be well represented by two straight lines with a marked break occurring at about C_{10}. However, when the products are considered on the basis of compound classes, the situation shown in Figure 8 is an oversimplification. As shown in Figure 10, Huff and Satterfield found that only the paraffins deviate from the ASF plot; oxygenates and alkenes appear to follow a single ASF plot with $\alpha \sim 0.55$.

Egiebor et al. (53) also reported that the break in the ASF plot was due to the alkanes. These authors showed that α-olefins and cis- and trans-β-olefins all show straight line plots with different slopes. They concluded that all these compounds are primary products. The fact that only paraffins show a break in the ASF slope proves that paraffins are not secondary products derived from α-olefins. These authors advanced the view that growth of linear chains proceed at the same rate (α) for all species and that it is the termination event which is species specific. The break in the paraffin ASF plot is therefore caused by a sharp change in the rate of termination at about C_{13}. Since a number of investigators have found that the carbon number where the break occurs is about the same and since the

break is observed with a variety of catalysts, they state that it may be that the phenomenon is governed by the nature of the C_{13} molecule as well as the catalyst.

Gaube and coworkers (54,55) also observed a two α plot. For an iron catalyst the C_3 - C_{40} products exhibit a linear ASF plot that only required a single α value (Figure 11). However, when the catalyst contained alkali (added as K_2CO_3), the ASF plot needed two α values to adequately describe the data. However, others have found the need for two alpha values for catalysts that do not contain potassium or other alkali metals (e.g., 56-59).

Donnelly et al. (60) extended the chain growth theory to include two growth probabilities; thus, rather than equation [4] one should write

$$m_p = AP\alpha^P + BP\alpha^P \qquad \textbf{[13]}$$

The contribution of each growing chain will be equal at the break point. They offer this as an improved equation for analyzing FTS product distributions, and show that this equation adequately described their data.

Dictor and Bell (56) found a two-alpha plot for both reduced and unreduced iron oxide catalysts. Furthermore, these authors found that the ASF plot for n-aldehydes yielded a two-alpha plot just as was the case for the hydrocarbon products. Furthermore, the break for the aldehydes was at the same carbon number as the hydrocarbons, provided the aldehyde ASF plot was based upon n-1 rather than n, as was used for the hydrocarbons (Figure 12). This was taken to support the view that aldehydes are formed by CO insertion into a growing surface alkyl group and subsequent reductive elimination of the acyl group (61,62); hydrocarbons on the other hand are believed to be formed in a termination step that occurs by elimination of a hydrogen from an alkyl group. Since the break occurs at n for hydrocarbons and n + 1 for the aldehydes, it appears that the oxygenate and hydrocarbon products are derived from a common surface species.

Donnelly and Satterfield (58) utilized a Ruhrchemie catalysts in a CSTR and found that both the n-alkanes and 1-alkenes fit a two-alpha ASF plot (Figure 12) whereas earlier work from that laboratory (52) showed that only n-alkanes deviated from ASF. In contrast to Dictor and Bell (56), Donnelly and Satterfield (58) found that oxygenates followed a single alpha plot even though they now find, in contrast to earlier results, that both n-alkanes and 1-alkenes deviate from ASF. These data serve to illustrate the difficulty in deciding the one or two-alpha plot question.

Stenger (63) showed that the two site ASF equation used by Huff and Satterfield was equivalent to one based on a distributed-site model in its ability to fit the molecular weight product distribution from an iron catalyst promoted with potassium. In the promoted catalyst, a distribution of sites proportional to the concentration of potassium relative to iron is utilized. In his model, Stenger assumed a normal distribution of K on the surface and postulated an exponential dependence of alpha on the random distribution variable, X, that is proportional to the potassium distribution.

Inoui et al. (64) introduced a single criterion to differentiate between the two-site model (58) and a distributed site model (63). However, for typical values of α_1 and α_2 for iron catalysts (~ 0.6 and 0.8, respectively) the fit to the ASF plot should make it difficult to distinguish the two models, even using the approach suggested by Inoui et al (64).

Kikuchi and Itoh (65) utilized an iron catalyst based upon ultrafine particles loaded with 1% K and found a break in the ASF plot at C_{10}. The data fit the model based upon two kinds of sites, A and B, with A exhibiting the lower and B exhibiting the higher growth probability. The fit of the experimental data and the calculated curve was satisfactory (Figure 13).

Iglesia et al. (66) reported that olefins readsorb and initiate surface chains that are indistinguishable from those formed directly from CO/H_2. Diffusion enhanced olefin readsorption leads to an increase in chain growth probability, α, and in paraffin content with increasing pore and bed residence time. Deviations from conventional (ASF) polymerization kinetics were quantitatively described by transport effects on the residence time of intermediate olefins within the liquid-filled catalyst pores without requiring the presence of several types of chain growth sites. The results reported for this study were obtained with a Ru catalyst, and not an iron catalyst.

Not all of the earlier studies require two or more α values to describe the distribution of products from FTS with iron catalysts. Three examples of this will be noted. Zwart and Vink (67) report that the product from zeolite supported iron catalysts derived from iron carbonyl complexes produced a product distribution in the C_{3-20} range which obeyed ASF statistics in all cases. Eilers et al. (68) report that in a few hundred independent FTS experiments with various catalyst formulations under different operating conditions it was confirmed that the carbon number distribution were in close agreement with the ASF kinetics (Figure 14). However, neither of the two data sets for the iron catalysts cover the total range of carbon numbers where the break in the ASF plot is observed. Cannella (69) reported a linear ASF plot that only required one alpha value to fit the C_{3+} products for an unsupported iron catalyst but that a two-alpha plot was required for the K-promoted catalyst. Linear ASF plots were always obtained for the C_3^+ products produced over each of the supported iron catalysts.

Tau et al. (70) found that a doubly promoted C-73 catalyst incorporated ^{14}C labeled 1-pentanol, added to the CO/H_2 feed, into higher carbon number products. They found that product accumulation in the CSTR was not adequate to explain the deviation from a constant ^{14}C activity/mole with increasing carbon number for higher carbon number alkane products.

^{14}C labeled ethanol served only as a chain initiator; this is demonstrated by the constant ^{14}C activity/mole for the C_2 through C_4 products (Figure 15). The constant activity of C_3 and C_4 that is equal to ethanol indicates that only one C_2 species derived from ethanol was incorporated into these products. These results are in agreement with the earlier data obtained by Emmett and coworkers (49, 71-75).

However, the data in Figure 16 clearly indicate that the C_{10} - C_{14} paraffins exhibit a different ^{14}C activity pattern with increasing carbon number than those in the C_2 - C_4 range. The higher carbon number products are diluted by the products accumulated in the reactor prior to the addition of ^{14}C labeled 1-pentanol. Analysis of the wax withdrawn from the reactor prior to the addition of the ^{14}C tracer provided data to calculate the impact of these products in diluting the ^{14}C content of higher carbon number products. Dilution did provide a minor contribution to the negative slope of the ASF plot in Figure 16; however, the points corrected for accumulation (◆) provided only a modest correction toward that exhibited by the lower carbon number products where ^{14}C/mole was constant with increasing carbon number (Figure 15). Hence, the effect of accumulation alone cannot account for the experimental data.

Another explanation for the deviation from the ASF plot is that hydrogenolysis of higher carbon number compounds produce more lower carbon number hydrocarbon products than can be accounted for by ASF. Using the same C-73 catalyst, Huang et al. (76) used octacosane, labeled at the carbon-14 position of the chain, to show that a detectable amount of hydrogenolysis did not occur even after one week of operation at the same conditions as was used by Tau et al. (70). Thus, hydrogenolysis is eliminated as an explanation for the two-alpha ASF plot for a promoted iron catalyst.

Tau et al. (70) concluded that the two alpha values in Figure 16 correspond to different product groupings. For the smaller alpha (about 0.62) the typical Fischer-Tropsch products are formed (alkanes, alkenes, oxygenates, etc.). However, for the larger alpha (about 0.82) the only significant product obtained corresponds to alkanes. The data in Figure 17, after first correcting for accumulation and then for the two different product groups, show a constant ^{14}C/mole, causing the conclusion based upon the higher carbon alkane products to be consistent with the one based on the lower alkane products.

In conclusion, it is evident that many groups using a variety of iron catalysts have found that two or more alpha values are needed if ASF kinetics are to account for the FTS products. The summary of the two-alpha values (77) for eight studies emphasize this conclusion. It is possible for deficiencies in the analytical determinations or loss of certain carbon number ranges during sampling or testing could cause the break in the ASF plot. However, this is not possible for the ^{14}C studies since the conclusion is based upon the ^{14}C/mole rather than the total number of moles. Recent data using ^{14}C-ethanol (78) and analysis of a wider carbon number range than in reference 32 provide additional support for the results reported by Tau et al. Furthermore, similar results are obtained for the addition of ^{14}C labeled C_2, C_3, C_5, C_6 and C_{10} alcohols and C_2, C_5 and C_{10} alkenes (79,80). With emphasis on the ^{14}C tracer studies, we conclude that it is likely that at least two chains are growing independently, and that these independent chains lead to different groups of products. These in turn require at least two-alpha values for the ASF to adequately describe the FTS data.

Supercritical Conditions

Several groups have reported results which indicate that operation in supercritical pressure conditions provides a means to significantly deviate from ASF product distributions(81-89). Much of the early work has been reviewed by Baiker (90). In summary, the use of supercritical conditions is viewed to limit secondary reactions, such as hydrogenation of the alkenes that are produced as primary products, but to enhance the secondary reactions of chain initiation by alkenes. Thus, when an alkene, e.g., 1-dodecene, is added together with the syngas feed, the added alkene initiates chains that produce additional high molecular weight products with the enhancement of the two-alpha distribution described above.

We have recently conducted supercritical FT synthesis using pentane plus hexane mixutres so that the density in the reactor could be varied from near gas-like to near liquid-like (91). Modeling of the supercritical fluid mixture indicated that an important increase in density occurs above a threshold of approximately 4 MPa for the reaction temperature of 220°C studied. While transport parameters of the fluid are largely retained, the observed improvement in wax solubility was noteable.

A cobalt catalyst (25%Co/γ-Al_2O_3) was used in a fixed bed reactor under a pressure/density tuned supercritical fluid mixture of n-pentane/n-hexane. By using inert gas as a balancing gas to maintain a constant pressure, the density of the supercritical fluid could be tuned near the supercritical point while maintaining constant space velocity within the reactor. The benefits of the mixture allowed for optimization of transport and solubility properties at an optimum reaction temperature for Fischer Tropsch synthesis with a cobalt catalyst. Indeed, above 4 MPa, increases in wax yields from sampling and carefully controlled gas measurements using an internal standard demonstrated an important increase in conversion due to greater accessibility to active sites after extraction of heavy wax from the catalyst. Additional benefits included decreased methane and carbon dioxide selectivities. Decreased paraffin/(olefin + paraffin) selectivities with increasing carbon number were also observed, in line with extraction of the hydrocarbon from the pore. Faster diffusion rates of wax products resulted in lower residence times in the catalyst pores, and therefore, decreased probability for readsorption and reaction to the hydrogenated product. Even so, there was not an observable increase in the alpha value for higher carbon number products over that obtained with just the inert gas.

The reason for the contradiction of the benefits of supercritical operations and deviations from ASF are not apparent. However, it is noted that those studies that reported non-ASF distributions were short-term experiments so that steady-state operations may not have been obtained.

The use of periodic pulsing of hydrogen and other gases to maximize C_{10}-C_{20} yield has been utilized (92). It was found that H_2 pulsing increased CO conversion significantly but only temporarily, with the activity gradually decreasing to the original value. Increasing the H_2 pulse frequency also increased both the CH_4 and C_{10}-C_{20} products. An optimal H_2-pulse frequency was required to maximize the yield of diesel-range FT products without substantially increasing the CH_4 yield. The potential of this type of operation to deviate from ASF distribution remains to be defined.

Summary

Both negative and positive deviations from the ASF distribution have been observed experimantally. To date, the author considers that the negative deviations have been obtained under conditions where experimental artifacts cannot be ruled out as causing the experimental observations. While it is more difficult to account for all of the reported positive deviations by experimental artifacts, it is considered to be likely that many of the observations are due to experimental conditions that do not account accurately for the impact of accumulation of heavier products in the reactor.

Note

This manuscript should be considered to be a work in progress. Prior to the AIChE meeting an updated version of the manuscript will be available at http://www.crtc.caer.uky.edu.

Acknowledgment

This work was supported with funding from the Commonwealth of Kentucky and the U.S. Department of Energy, Pittsburgh Energy Technology Center, through Contract No. De-AC22-84PC70029.

References

1. G. V. Schulz, *Z. Phys. Chem.*, **29**, 299 (1935); **30**, 375 (1935).
2. G. V. Schulz, *Z. Phys. Chem.*, **30**, 375 (1936).
3. P. J. Flory, *J. Amer. Chem. Soc.*, **58**, 1877 (1936).
4. E. F. G. Herrington, *Chem. Ind.*, (1946) 347.
5. R. A. Friedel and R. B. Anderson, *J. Amer. Chem. Soc.*, **72**, 1212 (1950); **72**, 2307 (1950).
6. S. Weller and R. A. Friedel, *J. Chem. Phys.*, **17**, 801 (1949).
7. R. B. Anderson, "The Fischer-Trospch Synthesis", Academic Press, New York, 1984.
8. B. Büssemier, C. D. Frohning, G. H. Horn and W. Kluy, German Offen. 2,518,964 and 2,536,488, 1976 (assigned to Ruhrchemie AG).
9. D. L. King,, J. A. Cusumano and R. L. Garten, Catal. Rev.-Sci, Eng., 23, 233 (1981).
10. R. J. Madon, E. R. Bucker and W. F. Taylor, US DOE Final Report, Contact No. E46-1-8008, July 1977.
11. R. J. Madon and W. F. Taylor in ACS Adv. Chem. Series (E. L. Kugler and W. F. Steffgen, Eds.) 178, 93 (1979).
12. R. J. Madon, J. Catal., 57, 183 (1979).
13. Catalytica Associates, Inc. 1980 Multiclient report.
14. T. P. Kobylinski and H. E. Swift; Hydrocarbon synthesis using a rare earth promoted metal silicate; U.S. 4,116,995, Sept. 26, 1978.
15. P. D. Caesar, J. A. Brennan, W. E. Garwood, and J. Ciric; Advances in Fischer-Tropsch Chemistry, J. Catal., 56, 274 (1979).
16. J. Eilers, J., S. Posthuma and S. Sie; Catal. Lett. 7 (l990) 253-270.
17. D. Vanhove, P. Makambo and M. Blanchard, J. Chem. Soc., Chem. Commun., (1979), 135.
18. H. H. Nijs, P. A. Jacobs, J. B. Uytterhoeven, J. Chem. Soc, Chem. Commun., 1979, 180, 1095.
19. D. Ballivet-Tkatchenko, N. D. Chau, H. Mozzanega, M. C. Roux and I. Tkatchenko in “Catalytic Activation of Carbon Monoxide,” (P. C. Ford, Ed.), ACS Symp. Series, 152, 187 (1981).
20. D. Frankel and B. C. Gates, J. Am. Chem. Soc., 102, 2478 (1980).
21. P. A. Jacobs and D. van Wouwe, J. Mol. Catal., 17, 145 (1982).
22. Th. Bein, G. Schmiester and P. A. Jacobs, J. Phys. Chem., 90, 4851 (1986).
23. T. J. Lee and B. C. Gates, Catal. Lett., 8, 15 (1991).
24. P.-L. Zhou, S. D. Maloney and B. C. Gates, J. Catal., 129, 315 (1991).
25. T. J. Lee and B. C. Gates, J. Mol. Catal., 71, 335 (1992).
26. S. Kawi, J. R. Chang and B. C. Gates, J. Catal., 142, 585 (1993).
27. S. Kawi, J.-R. Chang and B. C. Gates, J. Am. Chem. Soc., 115, 4830 (1993).
28. S. Kawi and B. C. Gates, J. Catal., 149, 317 (1994).
29. Y. Yang, K. Xie and X. Li in “Dynamics of Surfaces and Reaction Kinetics in Heterogeneous Catalysis, “ Studies in Surface Science and Catalysis, 109, 523 (1997).
30. R. P. K. Wells, P. J. Collier, M. Johns and G. J. Hutchings, DGMK Tagumgsbericht (2000) 2000-3, 111.
31. Y. Yang, S. Pen and B. Zhong, Catal. Lett., 16, 351 (1992).
32. H. H. Nijs and P. A. Jacobs, J. Catal., 65, 328 (1980).
33. M. A. McDonald, D. A. Storm and M. Boudart, J. Catal., 102, 386, (1986).
34. R. L. Espinoza and R. Snel, J. Chem. Soc., Chem. Commun., (1986), 1796.
35. T. Mitsudo, H. Boku, S. Murachi, A. Ishihara and Y. Watanabe, Chem. Lett., (1985) 1796.
36. V. K. Jones, L. R. Neubauer and C. H. Bartholomew, J. Phys. Chem., 90, 4832 (1985).
37. R. Snel, Catal. Lett., 1, 327 (1988).
38. R. K. Ungar and M. C. Baird, J. Chem. Soc., Chem. Commun., (1986), 643.
39. C. H. Bartholomew in “New Trends in CO Activation (L. Guczi, Ed.), Elsevier, Amsterdam, 1991, p 194.
40. D. Vanhove, Z. Zhuyong, L. Makambo and M. Blanchard, Appl. Catal., 9, 327 (1984).
41. K. C. McMahon, S. L. Suib, B. G. Johnson and C. H. Bartholomew, Jr., J. Catal., 106, 47 (1987).
42. D.-K. Lee and S.-K. Ihm, J. Catal., 106, 386 (1987).

43. G. A. Ozin, M. D. Baker and J. Godber in Heterog. Catal., Proc. Symp. Ind.-Univ. Coop. Chem. Program Dept. Chem., Texas A&M Univ., (B. L. Shapiro, Ed.), Texas A&M Univ. Press, College Station, TX, 1984, pp. 30-70.
44. L. F. Nazar, G. A. Ozin, F. Hugues, J. Godber and D. Rancourt, J. Mol. Catal., 21, 313 (1983).
45. L. F. Nazar, G. A. Ozin, F. Hugues, J. Godber and D. Rancourt, Angew. Chem., 95, 645 (1983).
46. R. B. Anderson in "Catalysis" (P.H. Emmett, ed.) Reinhold Pub. Corp., New York, 1956, Vol. IV, pp 22-256.
47. R. J. Madon and W. F. Taylor, *J. Catal.*, **69**, 32 (1981).
48. J. F. Schulz, W. K. Hall, B. Seligmon and R. B. Anderson, *J. Amer. Chem. Soc.*, **77**, 211 (1955).
49. W. K. Hall, R. J. Kokes and P. H. Emmett, *J. Amer. Chem. Soc.*, **82**, 1027 (1960).
50. S. Novak, R. J. Madon and H. Suhl, *J. Catal.*, **77**, 141 (1982).
51. C. N. Satterfield and G. A. Huff, Jr., *J. Catal.*, **73**, 187 (1982).
52. G. A. Huff, Jr. and C. N. Satterfield, *J. Catal.*, **85**, 370 (1984).
53. N. O. Egiebor, W. C. Cooper and B. W. Wojciechowski, *Canadian J. Chem. Eng.*, **63**, 826 (1985).
54. L. Konig and J. Gaube, *Chem. Ing. Tech.*, **55**, 14 (1983).
55. B. Schliebs and J. Gaube, *Ber. Bunsenges. Phys. Chem.*, **39**, 68 (1985).
56. R. A. Dictor and A. T. Bell, *J. Catal.*, **97**, 121 (1986).
57. L.-M. Tau, H. Dabbagh, B. Chawla and B. H. Davis, "Mechanism of Promotion of Fischer-Tropsch Catalysts", DOE/PC/70029-T1, Final Report, December 1987.
58. T. J. Donnelly and C. T. Satterfield, *Appl. Catal.*, **52**, 93 (1989).
59. H. Itoh, H. Hosaka and E. Kikuchi, *Appl. Catal.*, **40**, 53 (1988).
60. T. J. Donnelly, I. C. Yates and C. N. Satterfield, *Energy & Fuels*, **2**, 734 (1988).
61. H. Schulz and A. Zein El Deen, *Fuel Proc. Tech.*, **1**, 45 (1977).
62. P. Biloen, J. N. Helle and W. M. H. Sachtler, *J. Catal.*, **58**, 95 (1979).
63. H. G. Stenger, Jr., *J. Catal.*, **92**, 426 (1985).
64. M. Inoui, T. Miyake and T. Inui, *J. Catal.*, **105**, 266 (1987).
65. E. Kikuchi and H. Itoh, "Methane Conversion" (D. M. Bibby et al., eds.) Elsevier Sci. Pub., Amsterdam, 1988, pp 517-521.
66. E. Iglesia, S. C. Reyes and R. J. Madon, "Transport-Enhanced Olefin Readsorption Model of Hydrocarbon Synthesis Selectivity", 12th NAM of The Catalysis society, Abstract PC02, Lexington, KY, May 5-9, 1991.
67. J. Zwart and J. Venk, *Appl. Catal.*, **33**, 383 (1987).
68. J. Eilers, S. A. Posthuma and S. T. Sie, *Catal. Lett.*, **7**, 253 (1990).
69. W. J. Cannella, Ph.D. dissertation, U. of California, Berkeley, 1984.
70. L.-M. Tau, H. Dabbagh, S.-Q. Bao and B. H. Davis, *Catal. Lett.*, **7**, 127 (1990).
71. W. K. Hall, R. J. Kokes and P. H. Emmett, *J. Amer. Chem. Soc.*, **79**, 2983 (1957).
72. J. T. Kummer, T. W. DeWitt and P. H. Emmett, *J. Amer. Chem. Soc.*, **70**, 3632 (1948).
73. J. T. Kummer and P. H. Emmett, *J. Amer. Chem. Soc.*, **75**, 5177 (1953).
74. J. T. Kummer, H. H. Podgurski, W. B. Spencer and P. H. Emmett, *J. Amer. Chem. Soc.*, **73**, 564 (1951).
75. G. Blyholder and P. H. Emmett, *J. Phys. Chem.*, **63**, 962 (1959); **62**, 470 (1960).
76. C. S. Huang, H. Dabbagh and B. H. Davis, *Appl. Catal.*, **73**, 237 (1991).
77. D. K. Matsumoto and C. N. Satterfield, *Energy & Fuels*, **3**, 249 (1989).
78. Unpublished data.
79. L.-M. Tau, H. A. Dabbagh and B. H. Davis, *Energy & Fuels*, **5**, 174 (1991).
80. L.-M. Tau, H. A. Dabbagh and B. H. Davis, *Enertgy & Fuels*, **4**, 94 (1990).
81. K. Fujimoto, L. Fan and K. Yoshii,Topics in Catal., 2, 259-266 (1995).
82. L. Fan, K. Yokota and K. Fujimoto, Topics in Catalysis, 2, 267-283 (1995).
83. X. Lang, A. Akgerman and D. B. Bukur, Ind. Eng. Chem. Res., 34, (1995) 72-78.
84. D. B. Bukur, L. Xiaosu, A. Akgerman and Z. Feng, Ind. Eng. Chem. Res., 36 (1997) 2580-2587.
85. S. Yan, L. Fan, Z. Zhang, J. Zhou and K. Fujimoto, Appl. Catal. A: General, 171 (1998) 247-254.
86. N. Tsubaki, and K. Fujimoto, Fuel Processing Technology, 62, 173-186 (2000).
87. J. Zhou, J, S Yan, Z Gao and L Fan, Fuel Chem Preprint, 47 134 (2001).

88. X. Huang, C W Curtis and C B Roberts, Fuel Chem Preprint, 47, 150 (2002).
89. D. J. Bochniak, and B. Subramaniam, AICHE J., 44 (1998) 1889-1896.
90. A. Baiker, Chem Rev, 99 (1999) 453-473.
91. G. Jacobs, K. Chaudhari, D. Sparks, Y. Zhang, B. Shi, R. Spicer, T. K. Das, J. Li, and B. H. Davis, submitted.
92. A. A. Nikolopoulos, S. K. Gangwal and J. J. Spivey, Studies Surf. Sci. Catal., (Natural Gas Conversion VI), 136, 351, (2001).

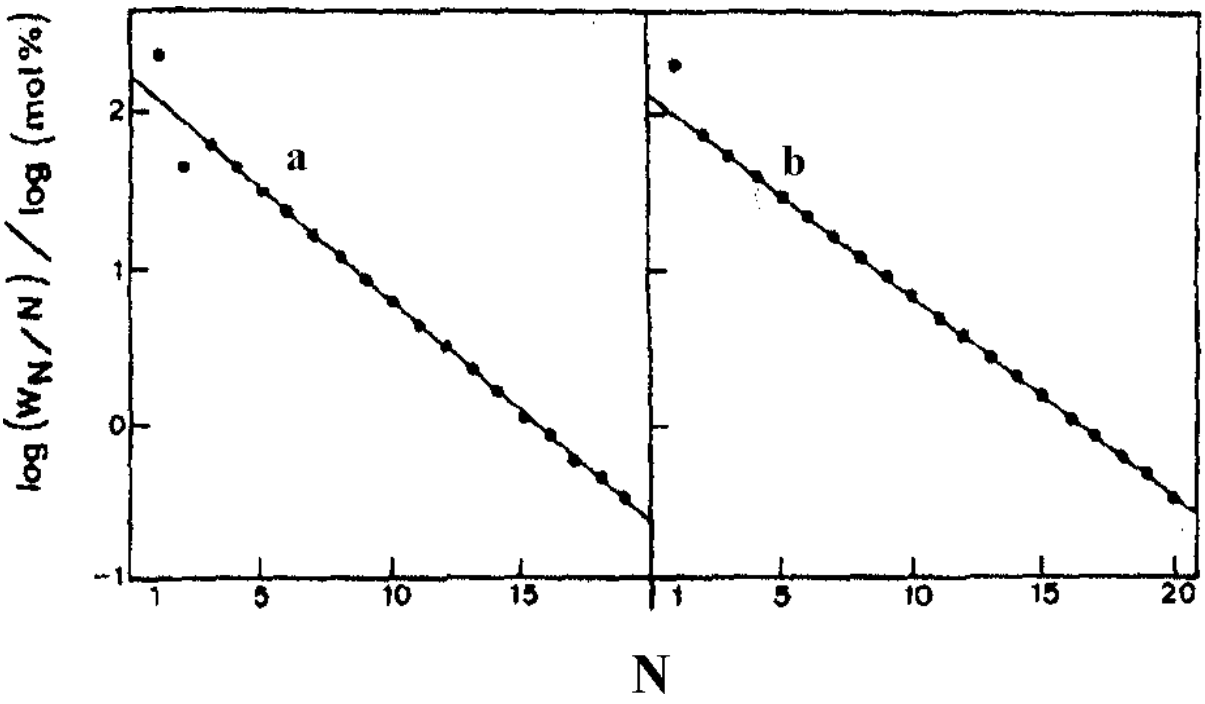

Figure 1. SF plot of the FT product distribution at steady-state obtained at 555 K for (a) Na-Y/FeO_4-RED and (b) Na-Y/Fe(O) after a time-on-streamof 60 and 54 h, respectively (from ref. 22).

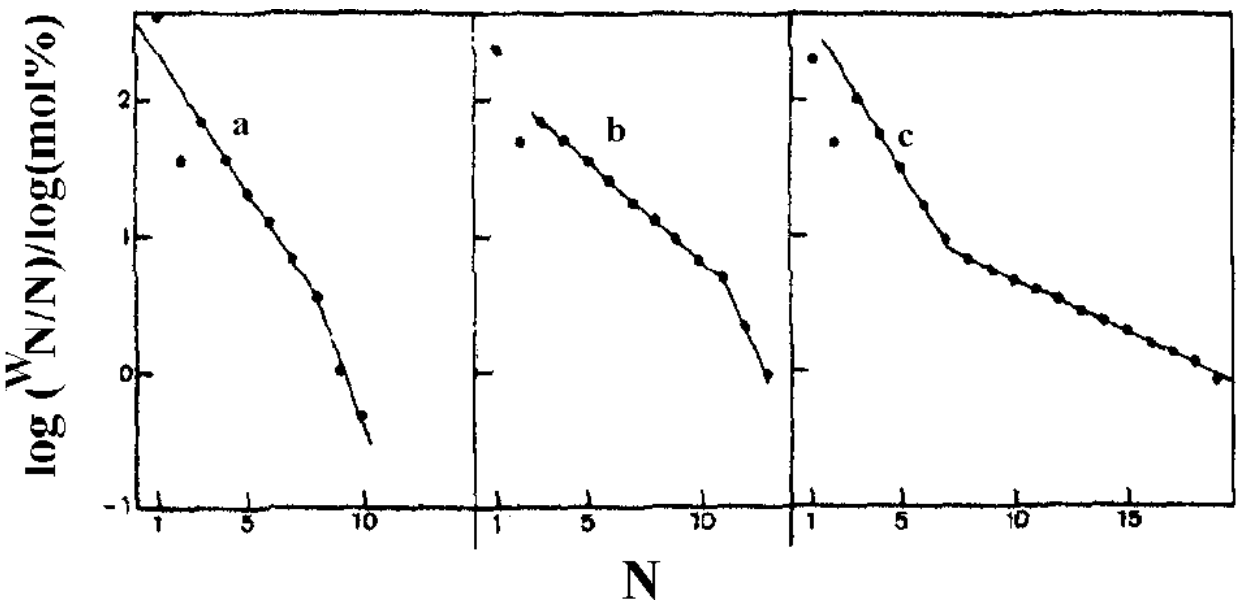

Figure 2. SF plot of the FT product distributions produced by iron Y zeolite catalyst with iron initially in the zeolite pores after (a) 0.5 h, (b) 15 h, and (c) 120 h time-on-stream (from ref. 22).

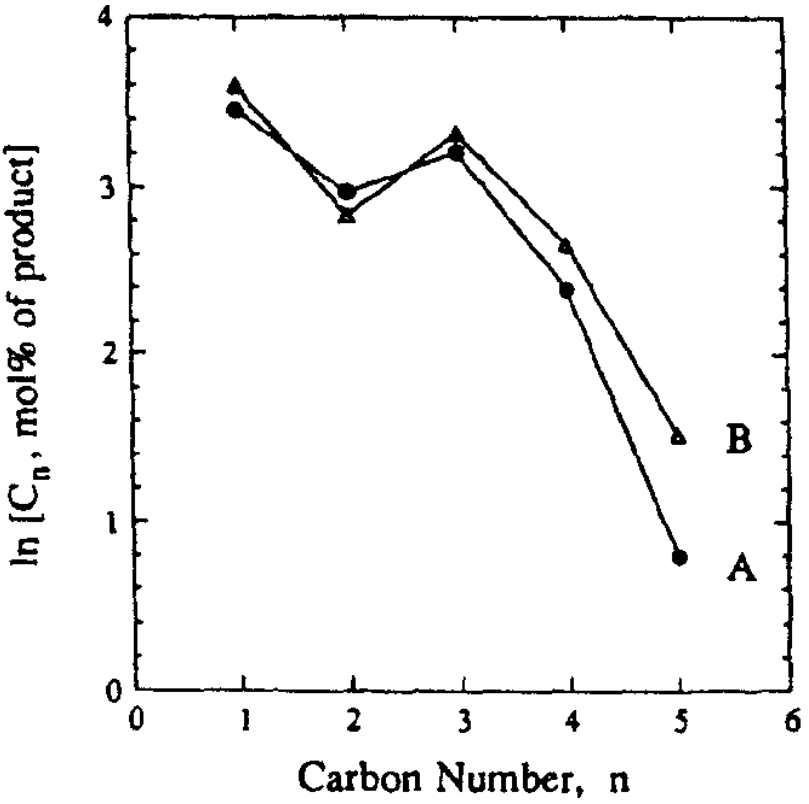

Figure 3. Hydrocarbon product distributions in CO hydrogenation catalyzed by zeolite-supported iridium carbonyl clusters: (A) 1 day on-stream and (B) 8 days on-stream (from ref. 27).

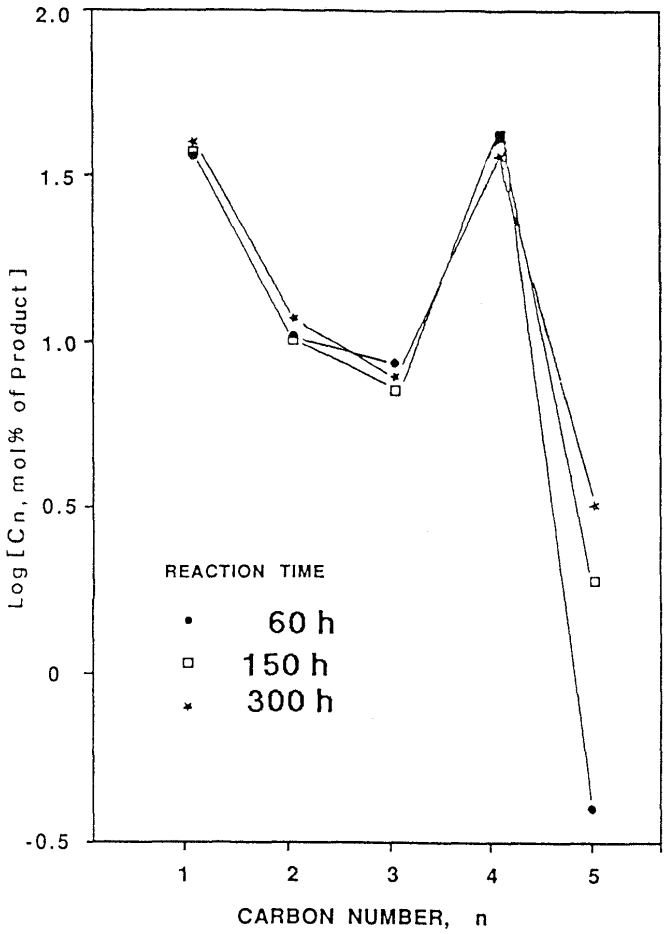

Figure 4. Hydrocarbon production distribution in CO hydrogenation catalyzed by zeolite-supported rhodium clusters (from ref. 23).

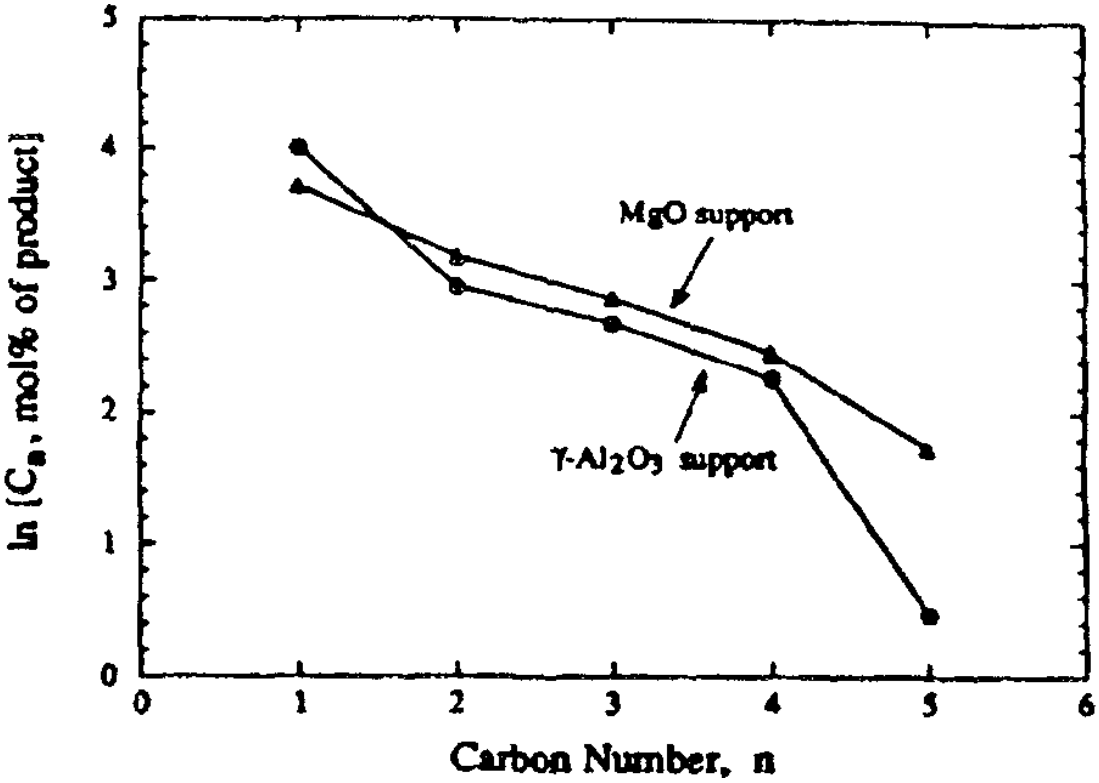

Figure 5. Hydrocarbon product distributions in CO hydrogenation (after 24 h) catalyzed by supported iridium samples (from ref. 28).

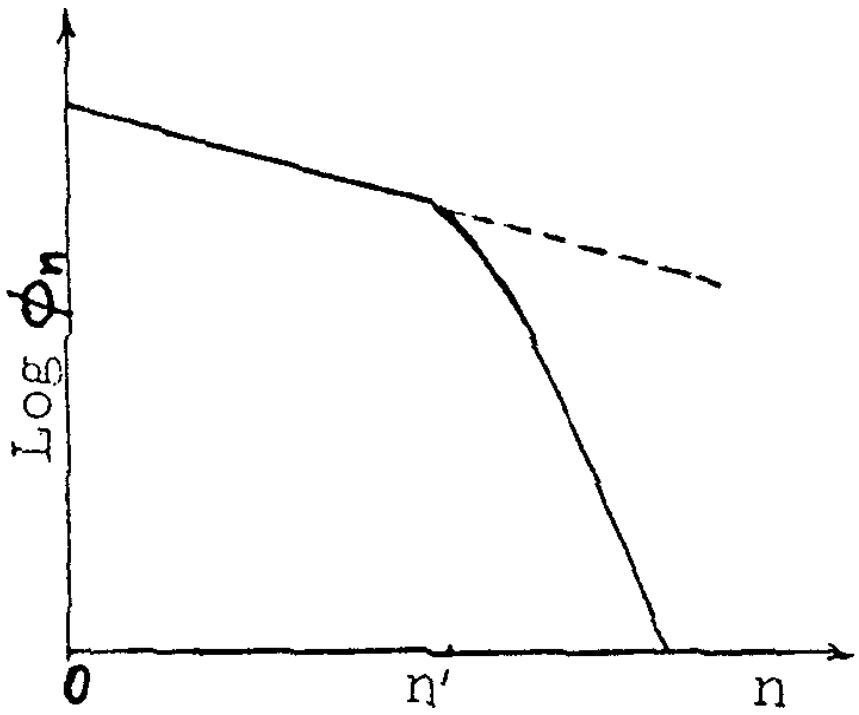

Figure 6. FT product distribution predicted by formula (3) for small crystallite metal catalysts (from ref. 31).

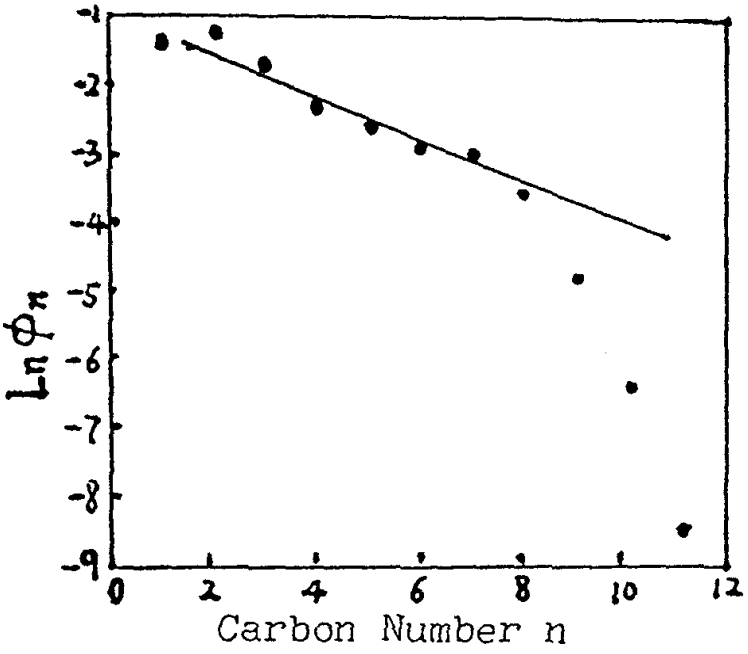

Figure 7. FT product distribution on 3% Fe/C (from ref. 31).

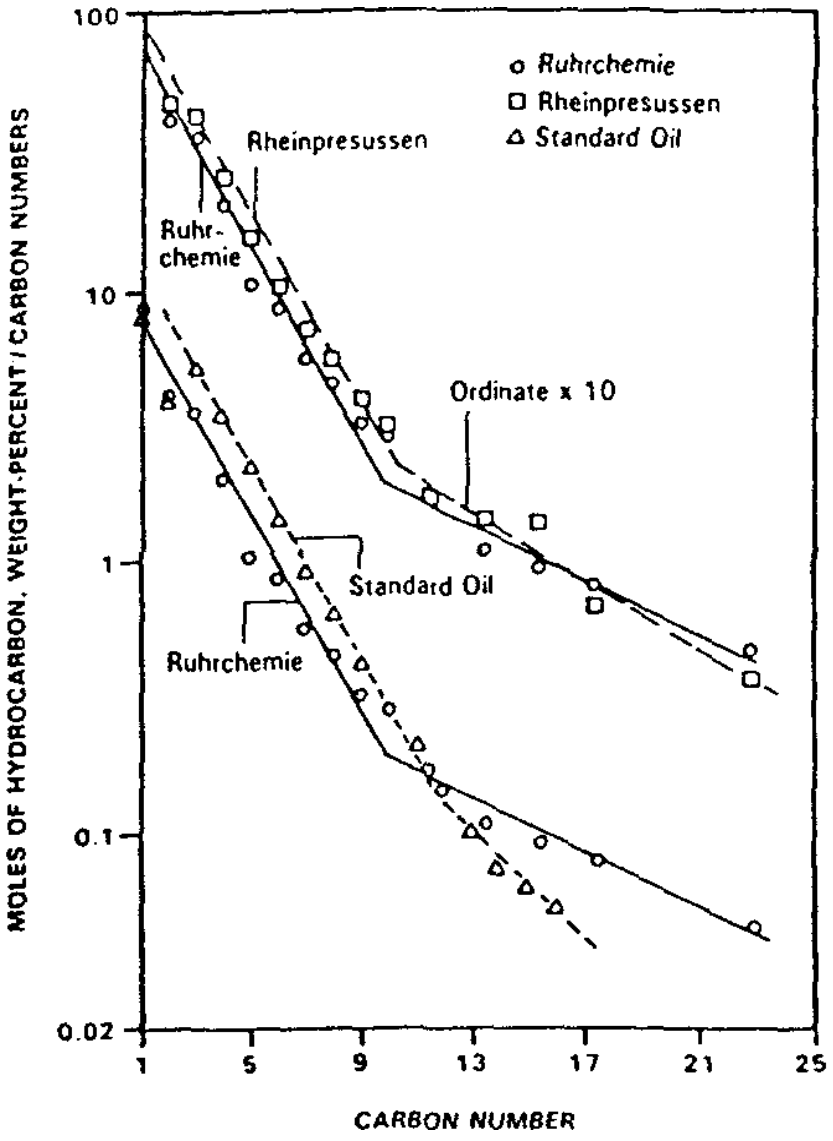

Figure 8. Anderson-Schulz-Flory (ASF) plots for the products from Schwarzheide for catalysts for four sources and Standard Oil Company of New Jersey (reproduced from ref. 46), p. 208).

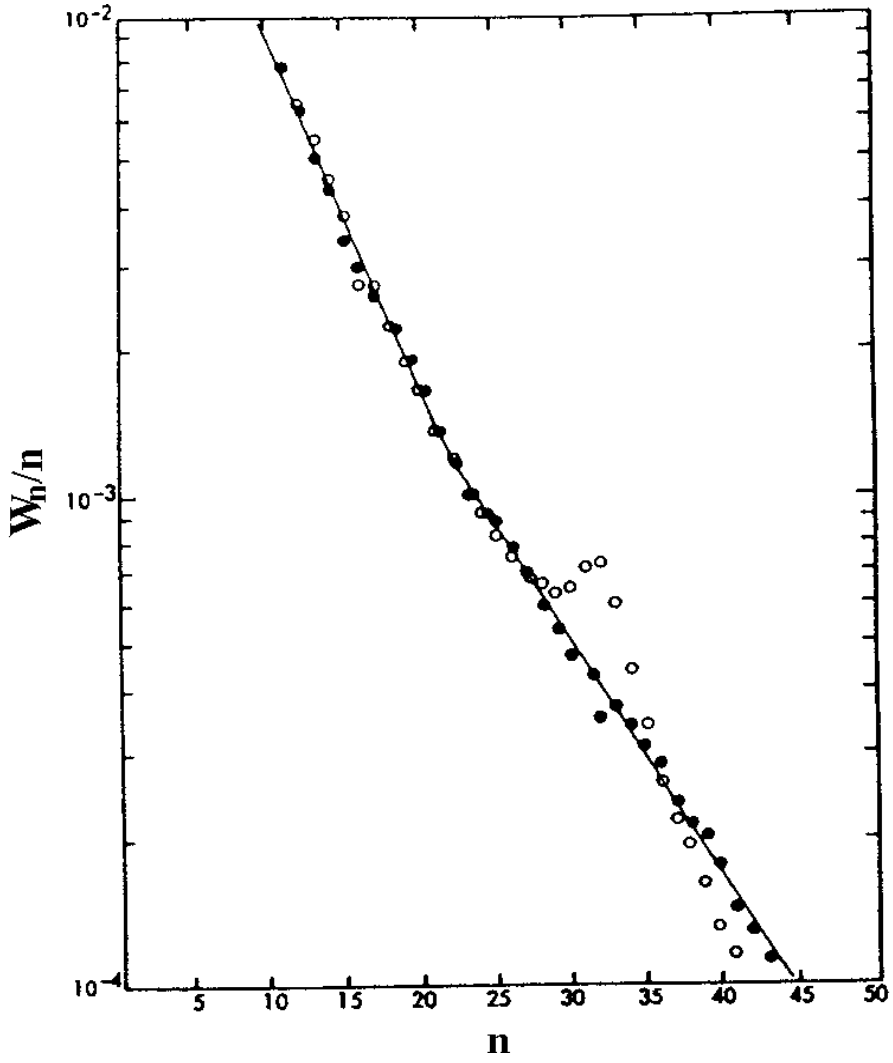

Figure 9. Plot of $\ell n\ W_n/n$ versus carbon number n. Open points, unsulfided catalysts; solid points, sulfided catalyst (reproduced from ref. 47).

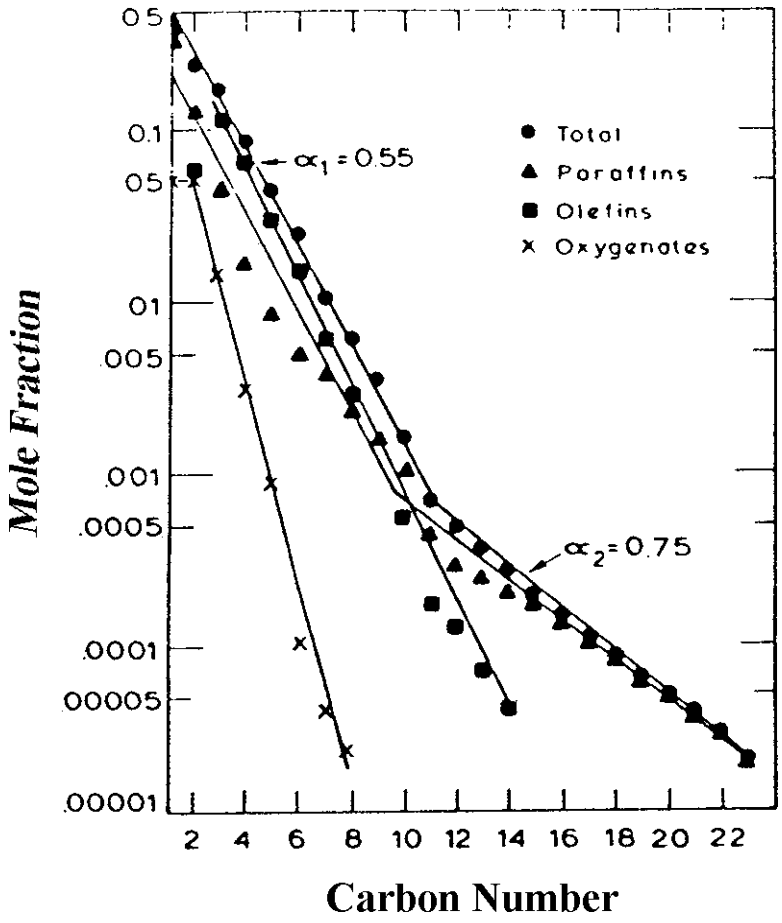

Figure 10. Flory distribution of MnO/Fe catalyst; 283°C, 1.24 MPa, $(H_2/CO)_m$ = 1.19 (reproduced from ref. 52).

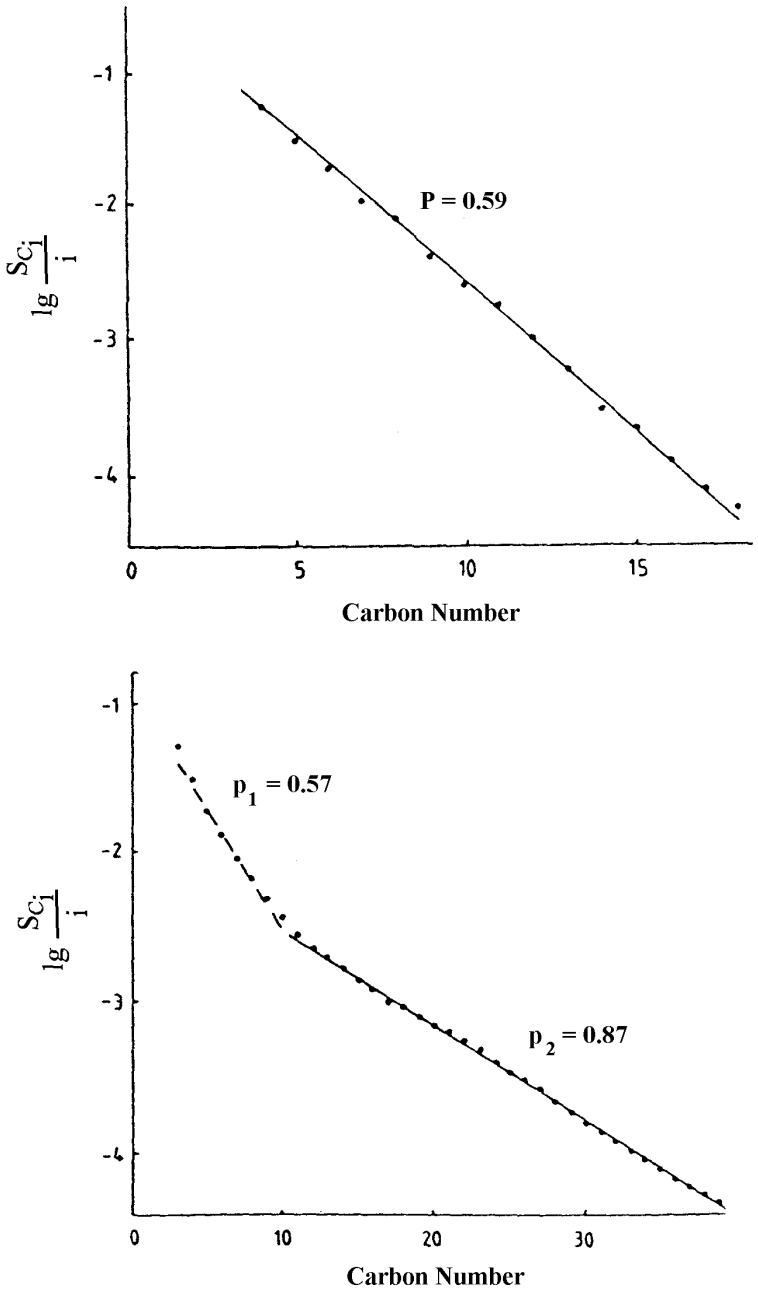

Figure 11. Product distribution from FTS using an iron (top) and potassium promoted iron catalyst (bottom) (redrawn from ref. 54).

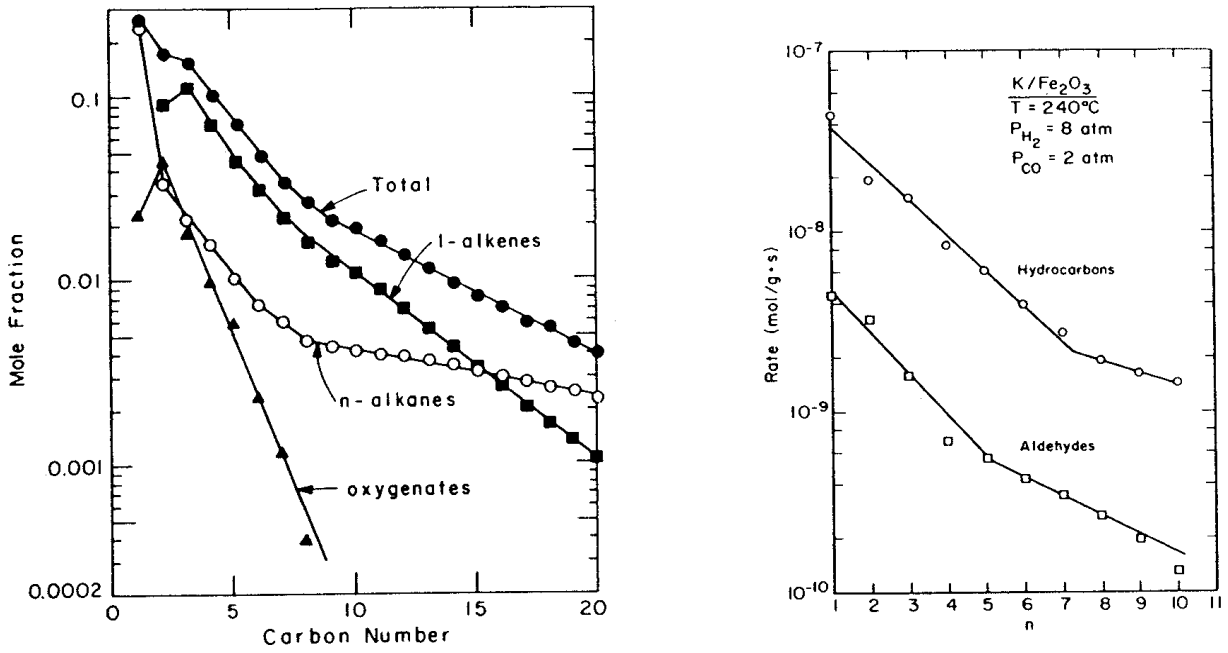

Figure 12. (left) Component Schulz-Flory diagram for overhead products. Ruhrchemie Catalyst MPa, 0.034 Nl/min/g_{cat}, $(H_2/CO)_{feed}$ = 0.7, 600 hours-on-stream (reproduced from ref. (20)). (right) Distribution of hydrocarbons and aldehydes from a common effluent sample. Each point for hydrocarbons represents the sum of 1-olefin plus n-paraffin; only straight-chain aldehydes are measured (reproduced from ref. 56).

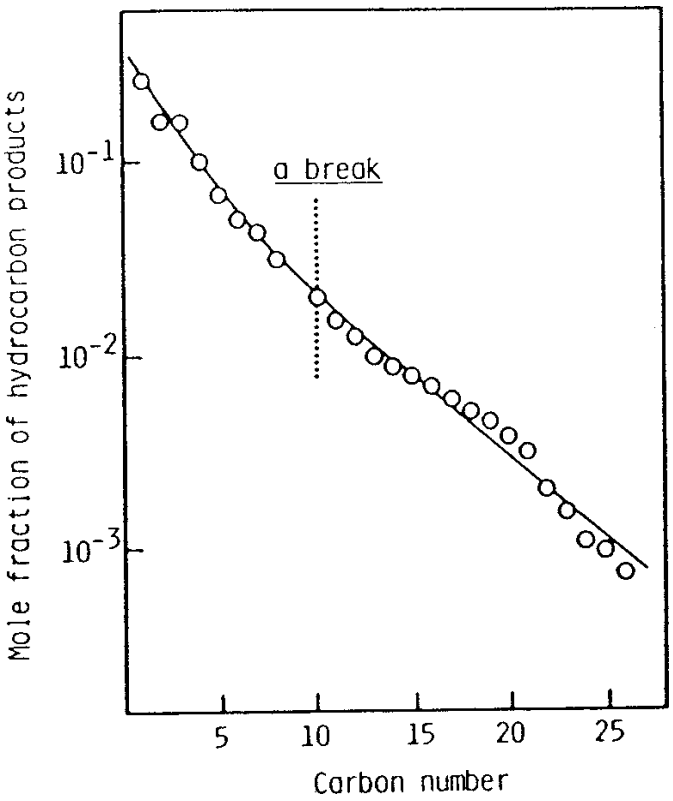

Figure 13. Flory plot of hydrocarbon products over potassium-promoted Fe UFP (ultrafine particle) catalyst. Reaction conditions: temperature, 220°C; pressure, 30 atm; H_2/CO, 1 mol/mol; W/F, 300 g-cat.min/CO-mol. Potassium addition: 1 wt.% of catalyst. Solid line represents the simulated distribution based on two-site ASF equation (reproduced from ref. 65).

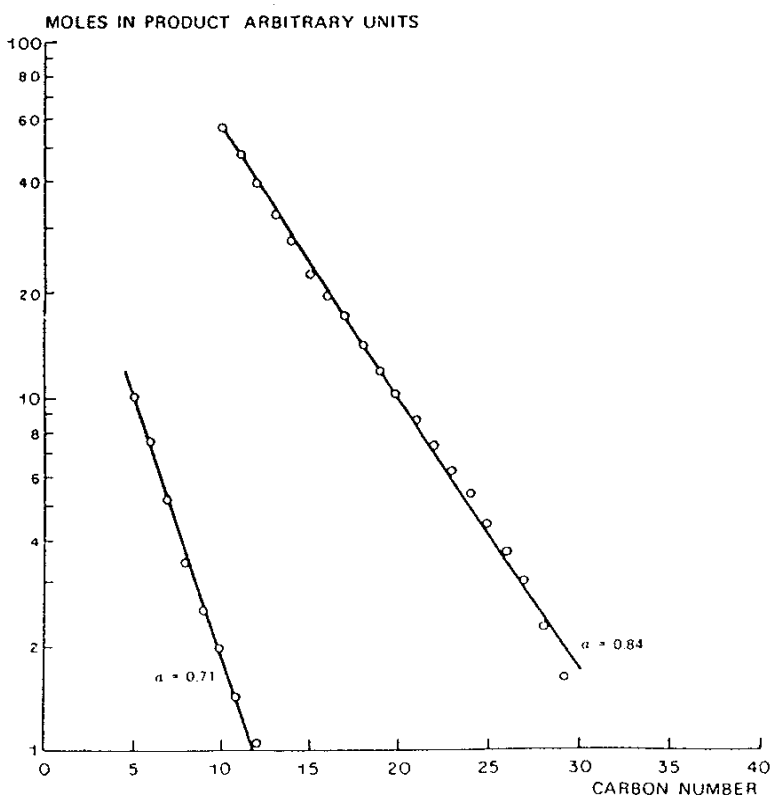

Figure 14. Typical carbon number distribution of the FTS using an iron catalyst (redrawn from ref. 67).

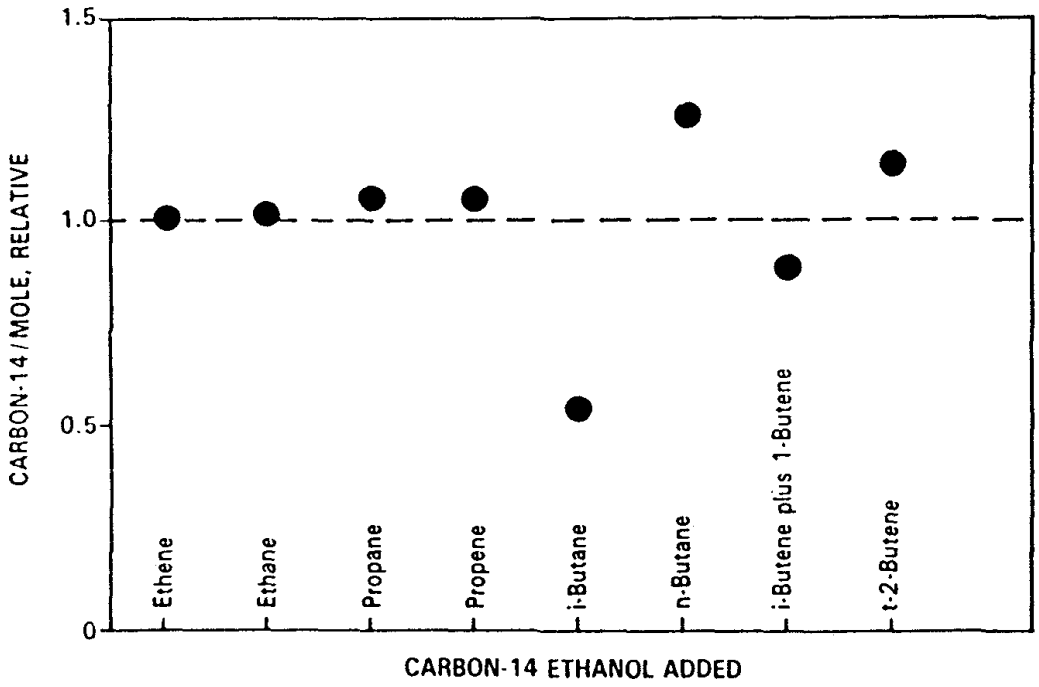

Figure 15. Relative ^{14}C/mole in gaseous products from the synthesis (7 atm, $H_2/CO = 1.2$, 262°C) with 3-volume % (based on alcohol and CO) [^{14}C-1]-ethanol was added during a 24 hour period (redrawn from ref. 70).

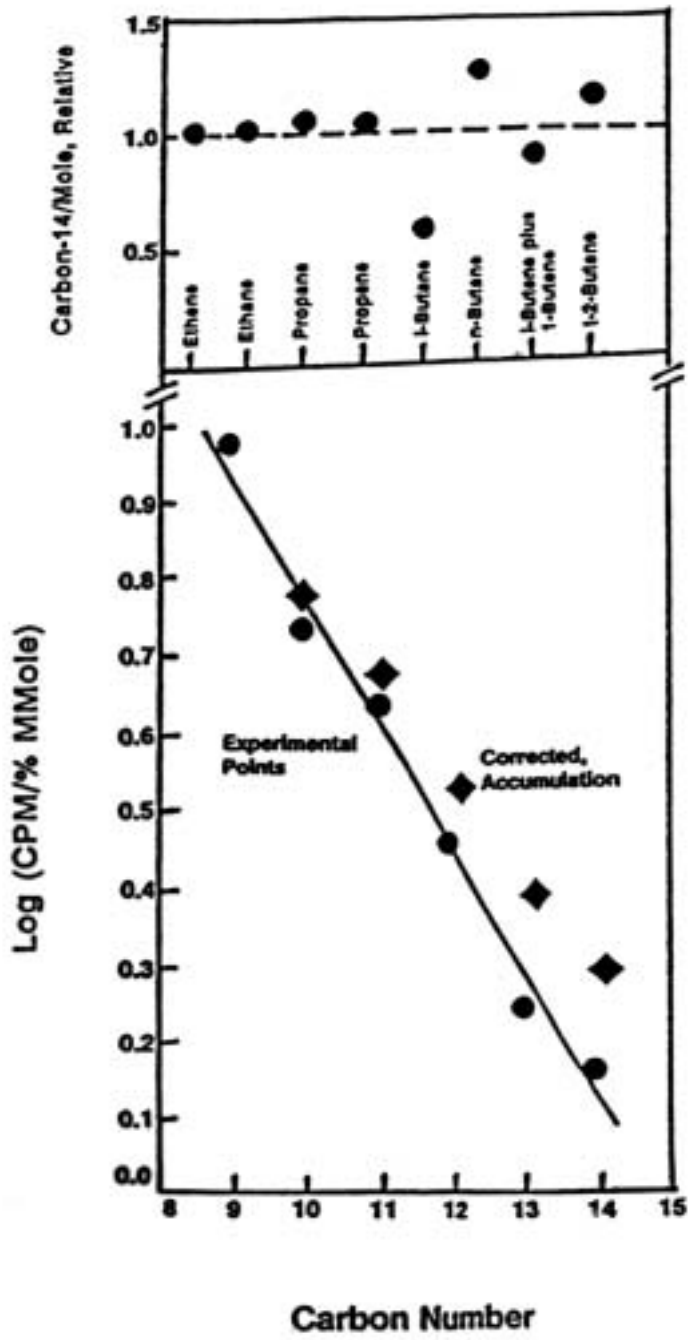

Figure 16. Composite figure showing relative radioactivity for the lower carbon number compounds (!); the measured values for the higher carbon number compounds (◆), and the values for the higher carbon number compounds (#) after correcting for reactor accumulation effects (redrawn from 70).

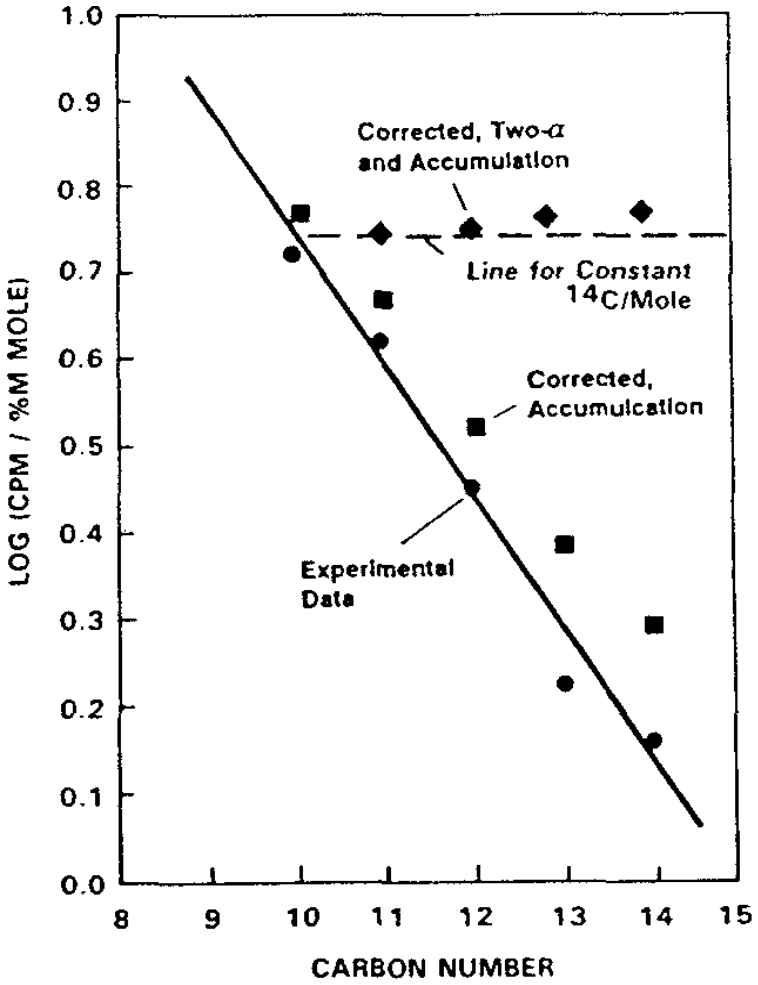

Figure 17. Radioactivity of the: alkane products (!); experimental data corrected for accumulation using data shown in Table 1 (#), and experimental data corrected for both accumulation and the two alpha mechanism (see text for details) (◆) (redrawn from ref. 70).